ISSN 1063-7842, Technical Physics, 2011, Vol. 56, No. 5, pp. 701–707. © Pleiades Publishing, Ltd., 2011.
Original Russian Text © I.A. Lyashenko, 2011, published in Zhurnal Tekhnicheskoĭ Fiziki, 2011, Vol. 81, No. 5, pp. 115–121.

SURFACE, ELECTRON AND ION EMISSION

Tribological Properties of Dry, Fluid, and Boundary Friction

I. A. Lyashenko

Sumy State University, ul. Rimskogo-Korsakova 2, Sumy, 40007 Ukraine
e-mail: nabla04@ukr.net

Received August 5, 2010

Abstract—A friction pair is studied under lubricant-free dry friction, hydrodynamic, and boundary lubricant conditions. It is shown that, in dry friction, the number of harmonics in the time dependence of the coordinate of the lower rubbing block decreases with increasing frequency of an applied periodic action until the interacting surfaces stick when a critical frequency is exceeded. The surfaces then move together. The behavior of a friction pair with a lubricant made of a Newtonian fluid, pseudoplastic fluid, or dilatant non-Newtonian fluid is analyzed in the hydrodynamic case. It is found that a pseudoplastic fluid or a boundary lubricant leads a intermittent (stick-slip) friction mode, which is one of the main causes of fracture of rubbing parts, over a wide parametric range.

DOI: 10.1134/S1063784211050227

INTRODUCTION

The processes that occur during friction cannot be described in terms of the classical mechanics because of the complex physicochemical processes proceeding in the contact zone of rubbing bodies. General tribology considers the following four basic types of friction: dry friction, which exists during the interaction of rubbing bodies without additional layers or lubricants; fluid friction, which exists when a lubricant is present between rubbing bodies; mixed friction, where dry and fluid friction regions exist in the contact zone; and boundary friction, when the lubricant thickness is smaller than 10 atomic layers or two rubbing surfaces separated by a lubricant layer interact with each other due to asperities, roughness, and so on. Since boundary friction often appears during sliding friction [1], it requires a separate investigation.

On the one hand, an extremely thin lubricant layer in boundary friction gives no way of using a standard hydrodynamic ideology for its description; on the other hand, the complexity and diversity of this process hinder the development of a universal microscopic model. Therefore, researchers often use phenomenological models that can explain experimental results [2–5]. Molecular dynamics simulation methods are also widely used [6]. Although they obtain good results, the description of any specific experimental situation requires a particular set of equations, which makes it difficult to trace a general tendency. Moreover, computer simulation cannot now describe long-term processes because of computation limitations. With a phenomenological approach, we can bypass these difficulties and relate the parameters of microscopic theories to macroscopic measurements. It should be noted that the boundary friction mode has been extensively studied in recent years [7–10].

The authors of [4] proposed an approach that takes into account dynamic and shear melting of a boundary lubricant. This approach was used to study the effect of basic parameter fluctuations on a system [11–13] and to consider the cause of the hysteresis in melting of a lubricant layer [14]. However, this approach is qualitative and can only trace general tendencies in the behavior of the system. The purpose of this work is to study a certain tribological system under dry, fluid, and boundary friction conditions. The dry and boundary friction conditions are shown to exhibit similar behavior in spite of radically different descriptions.

DRY FRICTION

We consider the tribological system shown in Fig. 1. Here, two springs with stiffness coefficient K are connected to a block of mass M placed on rolls, whose rolling friction is neglected. The second block is located on the first block; load L is applied to the second block, and it moves due to external forces. In the presence of interaction forces between the interacting

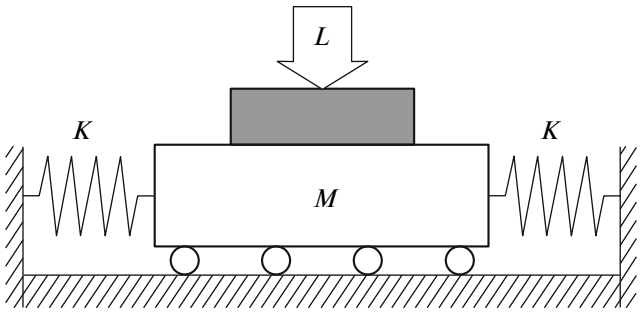

Fig. 1. Schematic diagram of the tribological system.

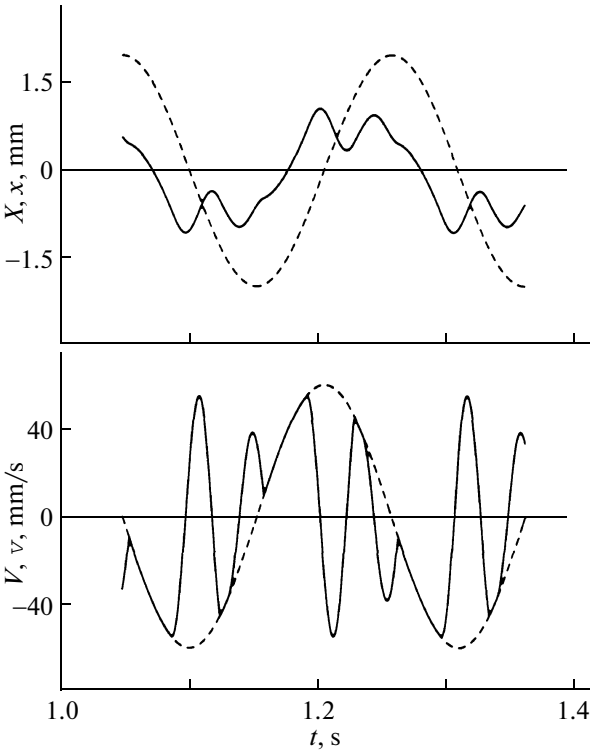

Fig. 2. Time t dependences of coordinates X, x and velocities V, v at parameters $A = 2 \times 10^{-3}$ m, $\omega = 30$ rad/s, $L =$ 20 N, $M = 0.6$ kg, $K = 7000$ N/m, and $\mu = 0.5$: (dashed lines) $X(t)$ and $V(t)$ and (solid lines) $x(t)$ and $v(t)$.

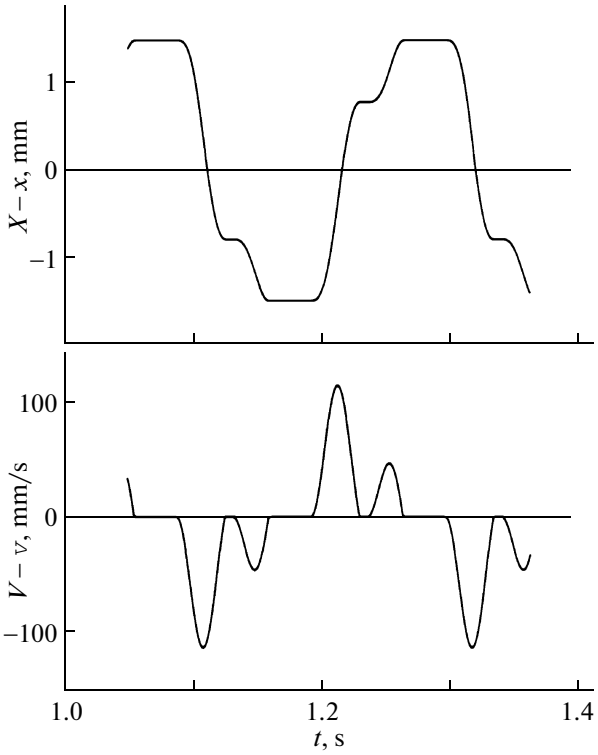

Fig. 3. Time t dependences of relative displacement $X(t) - x(t)$ and relative velocity $V(t) - v(t)$ of rubbing blocks corresponding to those in Fig. 2.

surfaces of these blocks, the lower block moves when the upper block moves, and the trajectory of the former depends on the friction mode. Such a setup was experimentally studied in [15], where a steel friction pair is used as interacting surfaces and ISO 32 paraffinic oil is used as a lubricant. The oil is continuously supplied to the contact zone at a fixed rate.

Let X and $V = \dot{X}$ be the upper block coordinate and velocity, respectively, and x and $v = \dot{x}$ be the lower block coordinate and velocity, respectively. We consider the case where the upper block is set in motion according to the cyclic law

$$X = A\cos(\omega t), \tag{1}$$

$$V = -A\omega\sin(\omega t), \tag{2}$$

where A is the amplitude and ω is the cyclic frequency. The equation of motion of the lower block is written in the form [15]

$$M\ddot{x} + 2Kx - F = 0, \tag{3}$$

where F is the friction force that moves the lower block. Since dry friction without a lubricant is analyzed, we assume that Amonton's law [1]

$$F = \mu L\,\mathrm{sgn}(V - v), \tag{4}$$

where μ is the friction coefficient, holds true. To take into account the force direction, we introduced the sign function defined in a standard manner,

$$\mathrm{sgn}(V - v) = \begin{cases} 1, & V > v \\ -1, & V < v \end{cases} \tag{5}$$

into Eq. (4). The result of numerical solution of Eqs. (1)–(5) is shown in Fig. 2. The dashed line in the upper panel shows the $X(t)$ dependence of the upper block coordinate (see Eq. (1)), and the solid line shows lower block coordinate $x(t)$. The $x(t)$ curve has additional harmonics, i.e., a more complex shape. The curves in the lower panel illustrate the time dependences of the block velocities. There are long time intervals in which these curves coincide; that is, the block velocities coincide. These situations correspond to the cases where the rubbing blocks "stick" to each other, and their relative displacement is absent. When velocities V and v do not coincide, the sliding friction mode takes place.

Figure 3 additionally shows the time dependences of the relative displacement of the blocks and their relative velocity. Here, in the time intervals of sticking, relative displacement $X - x$ remains constant and relative velocity $V - v$ is zero. Thus, a periodic stick–slip motion mode, which is characteristic of dry friction without a lubricant under certain conditions, takes place [1]. At the chosen parameters, the blocks stick to each other four times in a full period, i.e., two times in motion in each direction, and the obtained depen-

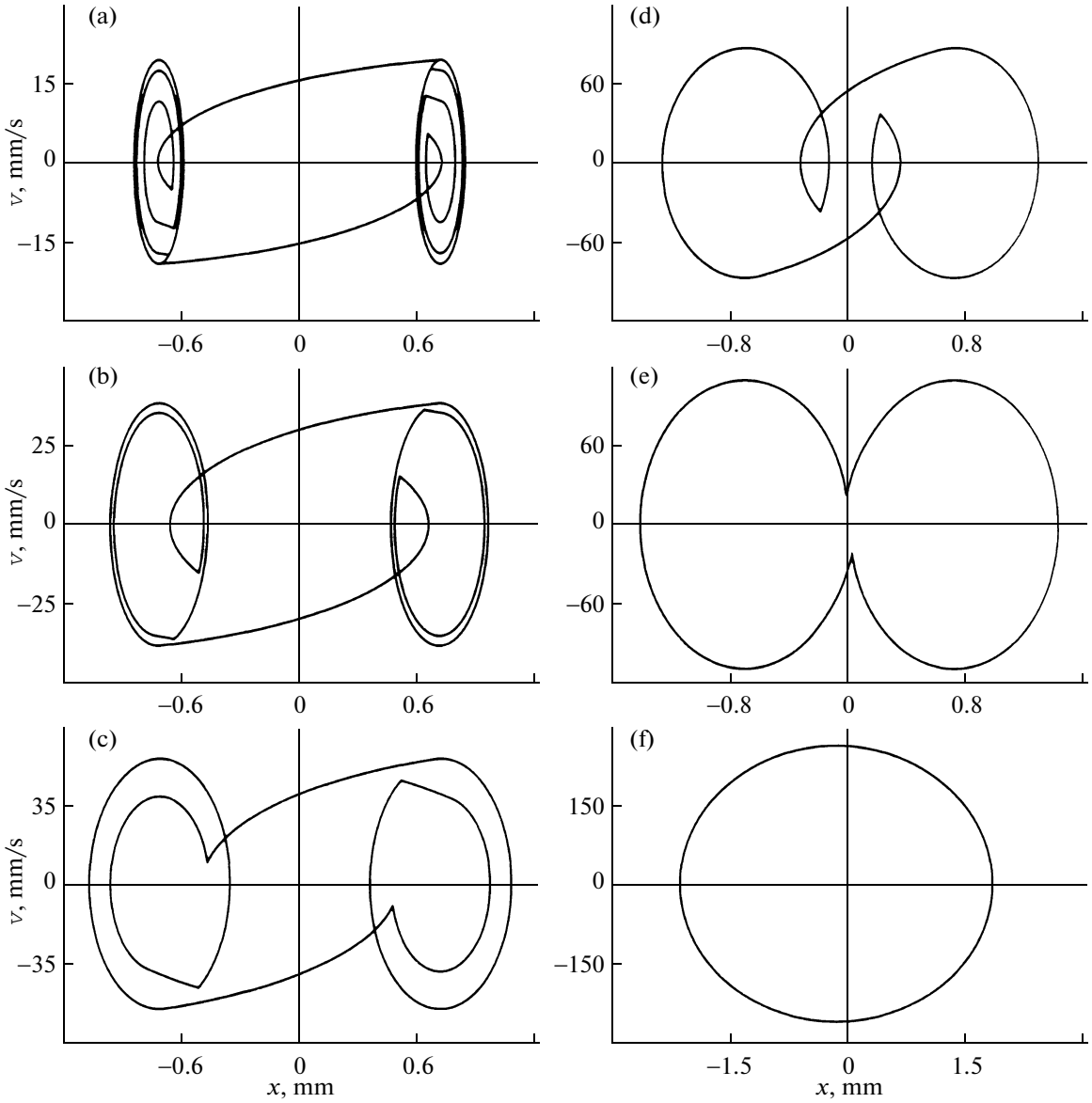

Fig. 4. Phase portrait of the system $\dot{x}(x)$ at the parameters of Fig. 2 and frequencies ω = (a–f) 10, 20, 30, 50, 80, and 130 rad/s, respectively. The number of harmonics decreases with increasing frequency.

dences are symmetric with respect to the motion direction. The dependences in Figs. 2 and 3 are shown under stationary conditions, and the system parameters do not change in time. In the calculations, we chose zero initial values and the dependences are given from a time $t = 5T$, where T is the period of function (1). In this time, a steady-state motion mode is reached. These dependences are shown for a time interval $\Delta t = 1.5T$.

Note that the behavior of the system depends strongly on load L applied to the upper block and frequency ω. The effect of these parameters and a number of other parameters on dry friction without a lubricant was experimentally studied in [16]; therefore, we will not dwell on this effect. Nevertheless, for generality, we present stationary dependences in the $\dot{x}(x)$ phase plane (or $v(x)$), which are absent in [16].

Figure 4 shows the phase portrait of the system at the parameters of Fig. 2 and various values of cyclic frequency ω. It is clearly visible that the behavior of the system becomes simpler as the frequency increases, since the total number of harmonics decreases. At a frequency $\omega = 130$ rad/s, the surfaces are stuck over the entire motion time, which is indicated by the shape of the corresponding phase portrait. It exhibits the periodic motion according to Eq. (1). Note that the third phase portrait was plotted at a frequency $\omega = 30$ rad/s, which corresponds to the curves shown in Fig. 2. Also note that all phase portraits apart from the last portrait, which illustrates the case of

complete sticking of the surfaces, are symmetric with respect to the origin of coordinates. This finding is related to the fact that the system at the initial stage changes in all cases where slip moments takes place and that a steady-state mode with symmetric dependences is reached. In this case, the surfaces are stuck at the beginning of motion and the entire subsequent time at $\omega = 130$ rad/s, which prevents the system from reaching a steady-state friction mode symmetric with respect to the shear direction. The behavior at any time depends on the initial position of rubbing blocks (initial conditions in equations), since this position remains the same in time.

FLUID FRICTION

If the two surfaces making up a friction pair are separated by a lubricant layer whose thickness is an order of magnitude larger than the microasperity height, we have a hydrodynamic mode. According to the Newtonian law, the friction force in this fluid mode is determined as [17]

$$F = \eta S\frac{V}{h}, \tag{6}$$

where η [Pa s] is the dynamic viscosity of the lubricant, S [m^2] is the contact area of the interacting surfaces, h [m] is the lubricant layer thickness, and V [m/s] is the viscous lubricant flow velocity. According to Eq. (6), the hydrodynamic friction force is independent of load L. However, the load also substantially affects the lubricant layer thickness and viscosity. The friction force in the hydrodynamic mode is approximately two orders of magnitude lower than the forces of boundary and dry friction, all other things being equal. It follows from Eq. (6) that force F is proportional to the relative shear velocity of the interacting surfaces; however, this situation takes place only for Newtonian fluids, whose viscosity η depends only on the properties of the lubricant and its temperature. In [18], we studied the effect of various temperature dependences of the viscosity on the boundary friction conditions in terms of a rheological model [4].

The viscosity of a non-Newtonian fluid during its flow depends also on the shear velocity gradient. Usually, these are heterogeneous fluids consisting of large molecules forming complex spatial structures, e.g., polymer lubricants, which are widely used in studying boundary friction [7]. To calculate the lubricant strain, we use the formula [17]

$$\dot\varepsilon = \frac{V}{h}, \tag{7}$$

where ε is the relative strain. Then, we can rewrite Eq. (6) in the form

$$F = \eta S\dot\varepsilon. \tag{8}$$

Usually, non-Newtonian fluids have complex $\eta(\dot\varepsilon)$ dependences. In particular, the viscosity of polymer solutions and melts usually decreases with increasing strain rate $\dot\varepsilon$ (so-called pseudoplastic fluids); however, the viscosity of a suspension of solid particles increases with $\dot\varepsilon$ (dilatant fluids). Therefore, for a qualitative analysis, we use the simple approximation [17]

$$\eta = k\dot\varepsilon^{\gamma}, \tag{9}$$

where coefficient of proportionality k [Pa s$^{\gamma+1}$] is introduced, in Eq. (8) and obtain

$$F = kS\dot\varepsilon^{\gamma+1} = kS\left(\frac{V}{h}\right)^{\gamma+1}. \tag{10}$$

Note that $\gamma < 0$ for pseudoplastic fluids, $\gamma > 0$ for dilatant fluids, and $\gamma = 0$ for Newtonian fluids (according to Eq. (9), the viscosity is independent of the velocity in this case).

For simulation, we use a formula for the friction force in the form

$$F = m\,\mathrm{sgn}(V - v)|V - v|^{\gamma+1}, \tag{11}$$

where we introduce the coefficient of proportionality

$$m = \frac{kS}{h^{\gamma+1}} \tag{12}$$

(measured in Pa s$^{\gamma+1}$ m$^{1-\gamma}$), sign function (5), and relative velocity $V - v$ of the interacting surfaces.

Figure 5 shows the time dependences of the velocity of the interacting blocks that were obtained as a result of the joint numerical solution of Eqs. (2), (3), (5), and (11). The three cases shown in Fig. 5 have the same parameters apart from coefficient γ. Therefore, we can analyze its effect on the behavior of the tribological system. In the first case (upper panel), a non-Newtonian pseudoplastic fluid ($\gamma = -2/3 < 0$) was chosen as a lubricant. For the chosen parameters, a stick–slip mode takes place. Note that pseudoplastic polymer lubricants are widely used for an experimental investigation of boundary friction [10, 17] and that they do exhibit the stick–slip mode in a certain parameter range [10]. In the case of a usual Newtonian fluid (central panel, $\gamma = 0$), the stable slip mode is reached, which is indicated by a low value of v, and the $v(t)$ dependence changes according to the sine law, as in the case of $V(t)$ but with a phase shift. Additional harmonics do not exist in the $v(t)$ curve, since friction force F (11) depends linearly on the relative surface shear velocity at $\gamma = 0$. Finally, in the last case (lower panel), a dilatant fluid ($\gamma = 2/3 > 0$) is used as a lubricant. The inset to Fig. 5 demonstrates that the $v(t)$ dependence in this case acquires a more complex shape because of the nonlinearity of Eq. (11); however, fluid friction occurs.

BOUNDARY FRICTION

In the previous sections, we analyzed the dry and hydrodynamic friction modes, whose considerations are similar and differ only in the dependences used to determine friction force F. In the case of boundary friction, the situation is not so simple, since the

description of the state of lubricant requires an individual theory. In this work, we use the model [19] based on the Landau theory of phase transitions [20]. One of the key points of this theory is the introduction of excess volume parameter f, which appears due to the chaotization of the structure of solids upon melting. When f increases, the defect density in a lubricant increases, and the lubricant passes into the kinetic mode of plastic flow (liquidlike phase) due to the transport of defects under applied stresses. Earlier, such an approach was used to describe severe plastic deformation processes [21–23].

We briefly present the main points of this theory, leaving aside heat conduction processes, spatial heterogeneity, and entropy factors. As a result, we substantially decrease the number of parameters only weakly changing the basic results. In addition, we take into account the load applied to the upper block. Although this point was not taken into account in [19], it has significant applied importance.

We first write the dependence of free energy Φ on excess volume f in the form

$$\Phi = \Phi_0 - \varphi_0 f + \frac{1}{2}\varphi_1 f^2 - \frac{1}{3}\varphi_2 f^3 + \frac{1}{4}\varphi_3 f^4, \qquad (13)$$

where we take into account the dependences on the invariants of strains ε_{ij}^e and lubricant temperature T for the lower expansion powers,

$$\Phi_0 = \Phi_0^* + \frac{1}{2}\lambda(\varepsilon_{ii}^e)^2 + \mu(\varepsilon_{ij}^e)^2, \qquad (14)$$

$$\varphi_0 = \varphi_0^* + \frac{1}{2}\bar{\lambda}(\varepsilon_{ii}^e)^2 + \bar{\mu}(\varepsilon_{ij}^e)^2 + \alpha T. \qquad (15)$$

Here, ε_{ii}^e and $(\varepsilon_{ij}^e)^2$ are the first and second strain tensor invariants [19, 24],

$$\varepsilon_{ii}^e = \frac{n}{\lambda_{\text{eff}} + \mu_{\text{eff}}}, \qquad (16)$$

$$(\varepsilon_{ij}^e)^2 = \frac{1}{2}\left[\left(\frac{\tau}{\mu_{\text{eff}}}\right)^2 + (\varepsilon_{ii}^e)^2\right], \qquad (17)$$

where n and τ are the normal and shear components of the stresses acting on the lubricant from the interacting surfaces.[1]

The elastic stresses are written as [19, 25]

$$\sigma_{ij}^e = \frac{\partial\Phi}{\partial\varepsilon_{ij}^e} = 2\mu_{\text{eff}}\varepsilon_{ij}^e + \lambda_{\text{eff}}\varepsilon_{ii}^e\delta_{ij}, \qquad (18)$$

where we introduce elastic parameters

$$\mu_{\text{eff}} = \mu - \bar{\mu}f, \qquad (19)$$

$$\lambda_{\text{eff}} = \lambda - \bar{\lambda}f, \qquad (20)$$

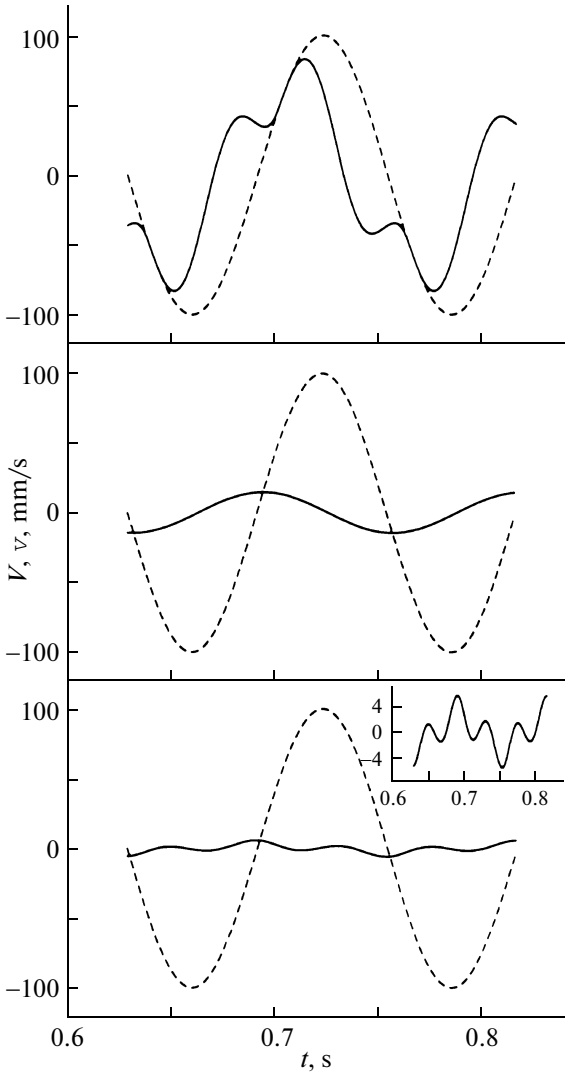

Fig. 5. Time t dependences of velocities V and v at parameters $A = 2\times10^{-3}$ m, $\omega = 50$ rad/s, $M = 0.6$ kg, $K = 5000$ N/m, and $m = 25$ Pa $s^{\gamma+1}$ $m^{1-\gamma}$. The panels located from top to bottom correspond to the values $\gamma = -2/3$, 0, 2/3: (dashed lines) upper block velocity V and (solid lines) lower block velocity v. The inset to the lower panel shows the enlarged $v(t)$ dependence.

which decrease with increasing f in melting.[2]

We then apply the principle of minimization of potential (13) and write an evolution equation for parameter f in the form of the Landau–Khlatnikov equation [20]. In an explicit form, this equation can be written as [19]

$$\tau_f\frac{\partial f}{\partial t} = \varphi_0 - \varphi_1 f + \varphi_2 f^2 - \varphi_3 f^3 - \frac{n^2(\bar{\lambda} + \bar{\mu})}{(\lambda_{\text{eff}} + \mu_{\text{eff}})^2}, \qquad (21)$$

[1] Shear stress τ is determined from Eq. (18) at $i \neq j$, i.e., $\delta_{ij} = 0$. In the case of $\mu_{\text{eff}} = 0$, term τ/μ_{eff} in Eq. (17) should be replaced by $2\varepsilon_{ij}^2$, according to Eq. (18).

[2] At $f > \mu/\bar{\mu}$, we should assume $\mu_{\text{eff}} = 0$; when $f > \lambda/\bar{\lambda}$, we should assume $\lambda_{\text{eff}} = 0$.

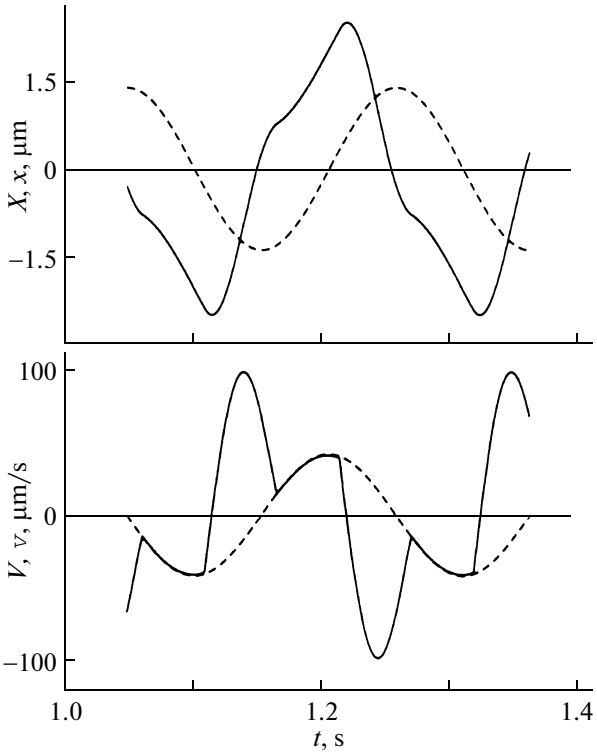

Fig. 6. Time t dependences of coordinates X, x and velocities V, v at parameters $A = 1.4 \times 10^{-6}$ m, $\omega = 30$ rad/s, $M = 0.7$ kg, $K = 1300$ N/m, $\gamma = -2/3$, $m = 0.05$ Pa $s^{1/3}$ $m^{5/3}$, $S = 3 \times 10^{-9}$ m, $n = -10^6$ Pa, and $T = 290$ K: (dashed lines) $X(t)$ and $V(t)$ and (solid lines) $x(t)$ and $v(t)$.

where relaxation time τ_f is introduced. The appearance of the last term in Eq. (21) is related to the dependence of invariants (16) and (17) on parameter f, and it is this dependence that takes into account the effect of an applied pressure.

As shown in [19], stationary elastic strain

$$\varepsilon_{ij}^{e} = \frac{(V - v)\tau_{\varepsilon}}{h}, \qquad (22)$$

where $V - v$ is the relative shear velocity and τ_ε is the Maxwell time of internal stress relaxation, appears in the lubricant layer during shear.

The friction force is determined as [19]

$$F = \tau S + m\,\mathrm{sgn}(V - v)|V - v|^{\gamma + 1}, \qquad (23)$$

where coefficient m is calculated from Eq. (12). Note that, as compared to hydrodynamic mode (10) and (11), an additional elastic component determined by the first term (τS) appears in Eq. (23) for the friction force in the boundary lubricant mode. It follows from Eqs. (18) and (22) that the sign of this term in Eq. (23) is taken into account automatically, which does not require the introduction of special sign function (5).

For further analysis, we use the experimental data from [10] and choose the following parameters [19]: $\Phi_0^* = 20$ J/m^3, $\lambda = 2 \times 10^{11}$ Pa, $\bar{\lambda} = 10^8$ Pa, $\mu = 4.1 \times 10^{11}$ Pa, $\bar{\mu} = 4 \times 10^{11}$ Pa, $\varphi_0^* = 5$ J/m^3, $\varphi_1 = 1100$ J/m^3, $\varphi_2 = 2700$ J/m^3, $\varphi_3 = 2070$ J/m^3, $\alpha = 0.45$ J K^{-1}/m^3, $h = 10^{-9}$ m, $\tau_f = 0.01$ Pa s, and $\tau_\varepsilon = 10^{-8}$ s.

We now analyze the kinetics of melting of a boundary lubricant in terms of the tribological model shown in Fig. 1. To this end, we simultaneously solve Eqs. (1)–(3), (5), and (15)–(23). The corresponding time dependences of the coordinates and velocities are shown in Fig. 6. They exhibit the stick–slip mode characteristic of boundary friction [10]. The behavior of the system in this case is analogous to that shown in Fig. 2 for dry friction without a lubricant. The only difference is that, in the case of boundary friction, the oscillation amplitude of the lower block is larger than the amplitude of the upper block, which sets the motion, at the chosen parameters. The response of a rubbing system to an external action that is similar to that shown in the upper panel in Fig. 6 was obtained in [2]. This shape in [2] was related to the presence of the third harmonic in the lubricant, which was established experimentally [9]. The advantage of the situation considered in this section over the situations considered above is that this model takes into account the effect of the lubricant temperature and the load applied to the friction surface. In particular, the authors of [19] analyzed the effect of temperature during shear of the upper interacting surface at a constant velocity and predicted the stick–slip mode obtained in this work in the hysteresis region.

CONCLUSIONS

With the proposed approach, we can describe the effects that occur during the friction of two surfaces under dry, fluid, and boundary friction conditions. A periodic stick–slip mode of melting/solidification of a lubricant is shown to take place in all situations. In particular, this mode occurs under hydrodynamic conditions over a wide parametric range for pseudoplastic non-Newtonian fluids, in which viscosity decreases with increasing velocity gradient. Our consideration makes it possible to trace the general tendencies in the behavior of rubbing systems operating under radically different friction conditions.

REFERENCES

1. B. N. J. Persson, *Sliding Friction: Physical Principles and Applications* (Springer, Berlin, 2000).
2. V. L. Popov, Zh. Tekh. Fiz. **71** (5), 100 (2001) [Tech. Phys. **46**, 605 (2001)].
3. J. M. Carlson and A. A. Batista, Phys. Rev. E **53**, 4153 (1996).
4. A. V. Khomenko and O. V. Yushchenko, Phys. Rev. E **68**, 036110 (2003).
5. A. E. Filippov, J. Klafter, and M. Urbakh, Phys. Rev. Lett. **92**, 135503 (2004).

6. O. M. Braun and A. G. Naumovets, Surf. Sci. Rep. **60**, 79 (2006).
7. J. Israelachvili, Surf. Sci. Rep. **14**, 109 (1992).
8. A. L. Demirel and S. Granick, J. Chem. Phys. **109**, 6889 (1998).
9. G. Reiter, A. L. Demirel, J. Peanasky, L. L. Cai, and S. Granick, J. Chem. Phys. **101**, 2606 (1994).
10. H. Yoshizawa and J. Israelachvili, J. Phys. Chem. **97**, 11 300 (1993).
11. A. V. Khomenko, I. A. Lyashenko, and V. N. Borisyuk, Ukr. Fiz. Zh. **54**, 1139 (2009).
12. A. V. Khomenko and Ya. A. Lyashenko, Zh. Tekh. Fiz. **80** (1), 27 (2010) [Tech. Phys. **55**, 26 (2010)].
13. A. V. Khomenko, I. A. Lyashenko, and V. N. Borisyuk, Fluct. Noise Lett. **9**, 19 (2010).
14. A. V. Khomenko and I. A. Lyashenko, Phys. Lett. A **366**, 165 (2007).
15. C.-R. Yang, Y.-C. Chiou, and R.-T. Lee, Tribol. Int. **32**, 443 (1999).
16. C.-R. Yang, R.-T. Lee, and Y.-C. Chiou, Tribol. Int. **30**, 719 (1997).
17. G. Luengo, J. Israelachvili, and S. Granick, Wear **200**, 328 (1996).
18. A. V. Khomenko and I. A. Lyashenko, Cond. Matt. Phys. **9**, 695 (2006).
19. I. A. Lyashenko, A. V. Khomenko, and L. S. Metlov, Zh. Tekh. Fiz. **80** (8), 120 (2010) [Tech. Phys. **55**, 1193 (2010)].
20. L. D. Landau and E. M. Lifshitz, *Course of Theoretical Physics*, Vol. 5: *Statistical Physics* (Nauka, Moscow, 1995; Pergamon, Oxford, 1980), Part 1.
21. L. S. Metlov, Metallofiz. Noveishie Tekhnol. **29**, 335 (2007).
22. L. S. Metlov, Izv. Ross. Akad. Nauk, Ser. Fiz. **72**, 1353 (2008).
23. L. S. Metlov, Phys. Rev. E **81**, 051121 (2010).
24. L. M. Kachanov, *The Bases of Plasticity Theory* (Nauka, Moscow, 1969) [in Russian].
25. L. D. Landau and E. M. Lifshitz, *Course of Theoretical Physics*, Vol. 7: *Theory of Elasticity* (URSS, Moscow, 2003; Pergamon, New York, 1986).

Translated by K. Shakhlevich